Editors' Suggestion | Featured in Physics

Hofstadter Topology: Noncrystalline Topological Materials at High Flux

Jonah Herzog-Arbeitman,[1,*] Zhi-Da Song,[1,*] Nicolas Regnault,[1,2] and B. Andrei Bernevig[1]
[1]Department of Physics, Princeton University, Princeton, New Jersey 08544, USA
[2]Laboratoire de Physique de l'Ecole normale supérieure, ENS, Université PSL, CNRS, Sorbonne Université, Université Paris-Diderot, Sorbonne Paris Cité, Paris 75005, France

(Received 1 July 2020; accepted 21 October 2020; published 2 December 2020)

The Hofstadter problem is the lattice analog of the quantum Hall effect and is the paradigmatic example of topology induced by an applied magnetic field. Conventionally, the Hofstadter problem involves adding $\sim 10^4$ T magnetic fields to a *trivial* band structure. In this Letter, we show that when a magnetic field is added to an initially *topological* band structure, a wealth of possible phases emerges. Remarkably, we find topological phases that cannot be realized in any crystalline insulators. We prove that threading magnetic flux through a Hamiltonian with a nonzero Chern number or mirror Chern number enforces a phase transition at fixed filling and that a 2D Hamiltonian with a nontrivial Kane–Mele invariant can be classified as a 3D topological insulator (TI) or 3D weak TI phase in periodic flux. We then study fragile topology protected by the product of twofold rotation and time reversal and show that there exists a higher order TI phase where corner modes are pumped by flux. We show that a model of twisted bilayer graphene realizes this phase. Our results rely primarily on the magnetic translation group that exists at rational values of the flux. The advent of Moiré lattices renders our work relevant experimentally. Due to the enlarged Moiré unit cell, it is possible for laboratory-strength fields to reach one flux per plaquette and allow access to our proposed Hofstadter topological phase.

DOI: 10.1103/PhysRevLett.125.236804

Introduction.—When a two dimensional crystalline lattice in which electrons have a trivial band structure is pierced by a uniform magnetic field, translational symmetry is broken and the energy spectrum develops a complex, fractal structure known as the Hofstadter Butterfly, which hosts a wealth of nontrivial Chern number topology despite the triviality of the original band structure [1–13]. In this Letter, we study the Hofstadter problem for an initially *topological* band structure and demonstrate new phases not possible in crystalline insulators. We prove that (1) a nonzero Chern number or mirror Chern number enforces a gapless point in the bulk of the Hofstadter Butterfly and (2) insulators with time-reversal symmetry $\mathcal{T}$ (TRS) and a nontrivial $\mathbb{Z}_2$ invariant can be considered as either strong or weak 3D topological insulators (TIs) in flux and host gapless edge states. We then study insulators with fragile topology protected by $C_{2z}\mathcal{T}$ symmetry and (3) show that the Hofstadter Hamiltonian can achieve a 3D higher order TI (HOTI) phase characterized by corner mode pumping. We then show that a model of twisted bilayer graphene (TBG) realizes the HOTI phase [14].

Recently, progress in the manufacture of two dimensional Moiré lattices with mesoscale effective unit cells has brought measurements of the Hofstadter Butterfly within reach by enabling access to large fluxes at laboratory-strength magnetic fields [14–26]. We expect our theoretical predictions to be verifiable in the near future, opening a new field of Hofstadter topology.

First, we review the framework for introducing magnetic flux on a lattice using the Peierls substitution [27]. We consider a general tight-binding model with unit vectors $\mathbf{a}_1$, $\mathbf{a}_2$ whose lattice points we call $\mathbf{R}$, with orbitals at $\boldsymbol{\delta}_\alpha, \alpha = 1, \ldots, N_{\text{orb}}$, and hopping elements given by $t_{\alpha\beta}(\mathbf{r}-\mathbf{r}'), \mathbf{r} = \mathbf{R} + \boldsymbol{\delta}_\alpha, \mathbf{r}' = \mathbf{R}' + \boldsymbol{\delta}_\beta$. The number of occupied bands is N_{occ}. We write $c^\dagger_{\mathbf{R},\alpha}$ ($c_{\mathbf{R},\alpha}$) as the fermion creation (destruction) operator of the α orbital at position $\mathbf{R} + \boldsymbol{\delta}_\alpha$. We find it convenient to work in units where the area of the unit cell, the electron charge e, and $\hbar$ are all set to one. By Peierls substitution, the hoppings acquire a phase $t_{\alpha\beta}(\mathbf{r}-\mathbf{r}') \to t_{\alpha\beta}(\mathbf{r}-\mathbf{r}')\exp[i\int_{\mathbf{r}'}^{\mathbf{r}} \mathbf{A}\cdot d\mathbf{r}]$. The path of integration is a straight line between the orbitals when they are well localized [28]. We work in the Landau gauge $\mathbf{A}(\mathbf{r}) = -\phi \mathbf{b}_1(\mathbf{r}\cdot\mathbf{b}_2)$ where the reciprocal vectors $\mathbf{b}_i$ satisfy $\mathbf{b}_i\cdot\mathbf{a}_j = \delta_{ij}$ and ϕ is the flux per unit cell. In this gauge, the hoppings retain translation invariance along $\mathbf{a}_1$, but the translation symmetry along $\mathbf{a}_2$ is broken. However, at rational values of the flux where $\phi = (2\pi p/q)$ with q, p coprime, the hoppings recover an extended translational symmetry: $\mathbf{r} \to \mathbf{r} + q\mathbf{a}_2$. In this case, we can diagonalize the Hamiltonian in the $1 \times q$ magnetic unit cell:

$$H^\phi = \sum_{k_1,k_2,\alpha,\beta,r_2,r_2'} c^\dagger_{k_1,k_2,r_2,\alpha}[\mathcal{H}^\phi(k_1,k_2)]_{r_2,\alpha,r_2',\beta} c_{k_1,k_2,r_2',\beta}. \quad (1)$$

Here $r_2', r_2 = 0, \ldots, q-1$ are the coordinates of the magnetic unit cell in the $\mathbf{a}_2$ direction, $k_1 \in (-\pi, \pi)$ is the

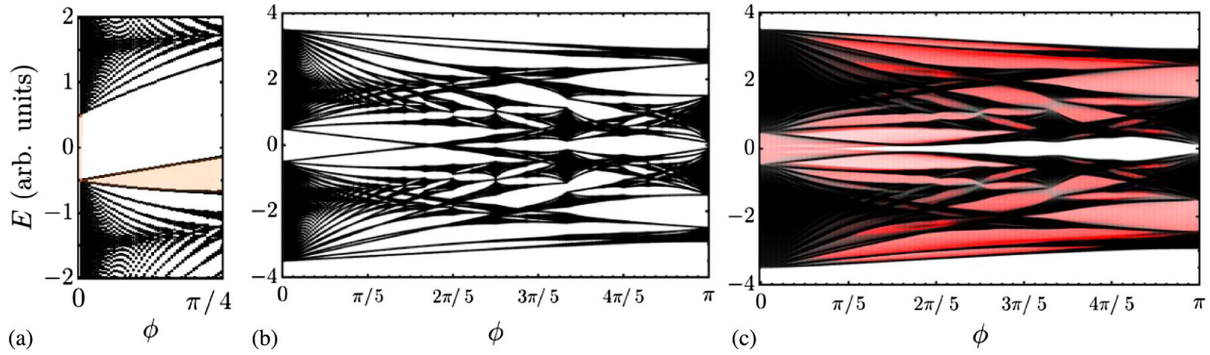

FIG. 1. Hofstadter butterflies. (a) We consider a $C = 1$ Chern insulator with the half filling many-body gap shaded in orange [28]. At zero flux, the gap is ~ 1, but when the flux is increased at constant filling, the gap discontinuously closes at infinitesimal ϕ. Notably, this discontinuity is impossible to realize in *any* crystalline system and relies on the infinitely large magnetic unit cell as $\phi \to 0$. (b) We consider the Hofstadter spectrum of a model H'_{QSH} with a nonzero mirror Chern number and all symmetries broken except for M_z and $\mathcal{T}$ [28]. The gap closing at finite ϕ is protected by M_z; breaking it allows a gap to open in the bulk. (c) We show the Hofstadter Butterfly calculated on a 30×30 lattice for H''_{QSH}, a variation where M_z is broken and $\mathcal{T}$ is the only symmetry [28]. The bulk spectrum (black) is gapped, but the edge spectrum (red) is gapless at $\phi = 0$. As the flux is increased to $\phi = \pi$, the edge states gap and move into the bulk. We also observe quantum Hall states at all fluxes and fillings where $\nu N_{\mathrm{orb}} \notin \mathbb{N}$. This is explained by the Diophantine equation, which can be written $(\phi/2\pi)C = N_{\mathrm{orb}}\nu \bmod 1$ [8].

momentum along $\mathbf{b}_1$, k_2 is the momentum along $\mathbf{b}_2$ and takes values in $(0, 2\pi/q)$ due to the enlargement of the magnetic unit cell, and $\mathcal{H}^\phi$ is the single-particle $qN_{\mathrm{orb}} \times qN_{\mathrm{orb}}$ Hamiltonian, which we will refer to as the Hofstadter Hamiltonian. Importantly, the Hofstadter Hamiltonian is periodic in flux up to a unitary transformation: $H^{\phi+\Phi} = UH^\phi U^\dagger$, where $\Phi = 2\pi n, n \in \mathbb{N}$ is determined by the condition that *all* closed hopping loops encircle an integer number of flux quanta. In simple models such as nearest-neighbor hopping on the square lattice, $n = 1$ [28]. We can show [28] that

$$U = \exp\left[i\sum_{\mathbf{R}\alpha}\int_{\mathbf{r}_0}^{\mathbf{R}+\boldsymbol{\delta}_\alpha} \tilde{\mathbf{A}}\cdot d\mathbf{r} c^\dagger_{\mathbf{R},\alpha}c_{\mathbf{R},\alpha}\right], \qquad \nabla\times\tilde{\mathbf{A}} = \Phi, \quad (2)$$

where $\mathbf{r}_0$ is the position of a fixed but arbitrary orbital of the Hamiltonian, and the integral may be taken along any sequence of Peierls paths due to the definition of Φ.

A central feature of the Hofstadter Hamiltonian is the increased periodicity of its Brillouin zone (BZ), which can be deduced from the magnetic translation group [29]. As shown in Eq. (1), k_2 is $2\pi/q$ periodic. Here we show that the energy bands are also $2\pi/q$ periodic along k_1. The single-particle magnetic translation operators are

$$T_i(\phi) = \sum_{\mathbf{R}\alpha} e^{i\int_{\mathbf{R}+\boldsymbol{\delta}_\alpha}^{\mathbf{R}+\boldsymbol{\delta}_\alpha+\mathbf{a}_i}\mathbf{A}\cdot d\mathbf{r} + i\chi_i(\mathbf{R}+\boldsymbol{\delta}_\alpha)} c^\dagger_{\mathbf{R}+\mathbf{a}_i,\alpha}c_{\mathbf{R},\alpha}, \quad (3)$$

where $\chi_i(\mathbf{r}) = \phi(\mathbf{a}_i \times \mathbf{r})\cdot\hat{z}$ has been determined by requiring $[H^\phi, T_i(\phi)] = 0$, and the integral is taken along a straight-line path [28]. While the translation operators commute in the absence of flux, otherwise we find $T_1(\phi)T_2(\phi) = e^{i\phi}T_2(\phi)T_1(\phi)$. However, at rational flux $\phi = (2\pi p/q)$, we see $[T_1(\phi), T_2^q(\phi)] = 0$. Hence $H^\phi, T_1(\phi)$, and $T_2^q(\phi)$ commute and eigenstates may be written as $|m, k_1, k_2\rangle$ with corresponding eigenvalues $\epsilon_m(\mathbf{k}), e^{ik_1}, e^{iqk_2}$, with $m = 1, \ldots qN_{\mathrm{orb}}$ [see Eq. (1)]. Because $[H^\phi, T_2(\phi)] = 0$, the states $T_2^j(\phi)|m, k_1, k_2\rangle$ also have energy $\epsilon_m(\mathbf{k})$. The k_1 momentum of such states is deduced from $T_1(\phi)(T_2^j(\phi)|m, k_1, k_2\rangle) = e^{i(k_1+j\phi)}T_2^j(\phi)|m, k_1, k_2\rangle$ and hence they represent the new states at $k_1 + j\phi$ [28]. Thus, we find

$$T_2^j(\phi)|m, k_1, k_2\rangle \sim |m, k_1 + j\phi, k_2\rangle, \quad j = 0, \ldots, q-1 \quad (4)$$

are all degenerate in energy. Recalling that $k_2 \in (0, 2\pi/q)$, we conclude that the magnetic BZ has an increased periodicity: $\epsilon_n(\mathbf{k}) = \epsilon_n[\mathbf{k} + (2\pi/q)\mathbf{b}_i]$, $i = 1, 2$. This feature is essential in the following proofs.

Chern insulators.—As a warmup, we study the Hofstadter Butterfly of a Chern insulator. According to the Streda formula [5], the filling of a state with fixed a nonzero Chern number changes as the flux is increased. In the paradigm of Hofstadter topology, we prove a complementary result: at *fixed* filling, the many-body gap of a Chern insulator has a discontinuity at $\phi = 0$ enforced by a mismatch between the Chern number at zero flux and any infinitesimal flux.

Consider a Hamiltonian $H^{\phi=0}$ that is gapped with a nonzero Chern number $C^{\phi=0}$ at filling $\nu = N_{\mathrm{occ}}/N_{\mathrm{orb}}$. We emphasize that we keep ν fixed as the flux is increased. Now we choose a flux $\phi = (2\pi p/q)$ such that $C^{\phi=0}/q \notin \mathbb{Z}$. The magnetic unit cell of H^ϕ contains qN_{orb} orbitals and qN_{occ} occupied bands at filling ν. First, we introduce an on-site potential term of overall amplitude M to $H^{\phi=0}$ that creates an energy splitting between each of the orbitals. For sufficiently large M,

the model will be split into N_{orb} trivial bands, and it will reach a gapped atomic limit for all ϕ [28,30,31].

As we tune M from zero to infinity, gap closings occur that eventually cause $H^{\phi=(2\pi p/q)}$ to undergo a series of phase transitions into a trivial atomic limit [28] at filling $\nu = qN_{\mathrm{occ}}/qN_{\mathrm{orb}}$ [32], recalling that the change in Chern number is determined locally by the closing bands [5,33,34]. If there is gap closing at $\mathbf{k}^*$, there must also be an *identical* gap closing at the each of the points $\mathbf{k}^* + j\phi\mathbf{b}_1 \mod 2\pi, j = 1, \ldots q-1$ due to the magnetic BZ periodicity of Eq. (4). Because a multiple of q gap closings separate H^ϕ from the trivial atomic limit at large M where the Chern number is zero, it must be that $C^{\phi=(2\pi p/q)\neq 0} \in q\mathbb{Z}$, zero included. Hence, we recover the result of Ref. [8] using a proof applicable to the next section.

Since we chose q such that $C^{\phi=0} \notin q\mathbb{Z}$, we find by construction that the Chern number has changed during an adiabatic perturbation of H^ϕ. But this is only possible if the gap closes for $\phi \in [0, (2\pi p/q)]$. For every $C^{\phi=0}$, we may choose an arbitrarily large q, allowing us to conclude that, at fixed filling, the many-body gap must close immediately when the flux is increased from the fine-tuned point at $\phi = 0$ [28]. This enforces a discontinuity in the occupied states as shown for a typical Chern insulator in Fig. 1(a). There is no protected gap closing if $C^{\phi=0} = 0$ because a vanishing Chern number is possible for all flux at filling $\nu = N_{\mathrm{occ}}/N_{\mathrm{orb}}$.

We now extend this result to insulators with a nonzero mirror Chern number [35,36]. Because mirror symmetry M_z is not broken in the presence of flux, M_z remains well-defined at all ϕ. Then we may block-diagonalize H^ϕ at all ϕ by its mirror eigenvalues. Each block has a nonzero Chern number at $\phi = 0$, and thus the gap closes immediately at $\phi = 0$ and filling ν within each individual block. Each block must have a branch of its spectrum connecting its valence and conduction bands. Hence for *any* Fermi energy in the zero-flux gap, there will be a gapless point at *finite* flux in the spectrum of the whole model [28]. In Fig. 1(b), we consider the quantum spin Hall model H_{QSH} of Ref. [35] with a nonzero mirror Chern number. We show numerical confirmation that, although the Chern number is identically zero due to TRS, the gap still closes due to the mirror Chern number.

Time-reversal invariant insulators.—We show in this section that when a Hofstadter Hamiltonian with spinful TRS $\mathcal{T}$ is topological (in a quantum spin Hall state) at $\phi = 0$, it realizes a nontrivial 3D phase where the flux ϕ is identified with k_z [35,37,38]. Recall that H^ϕ is $\Phi = 2\pi n$ periodic in flux. When n is odd, H^ϕ is classified as a 3D TI and may be a weak TI or 3D TI when n is even. However, it can never be 3D trivial.

The identification of ϕ with k_z is deduced from its transformation under $\mathcal{T}$. Because $\mathcal{T}$ is antiunitary, it flips the sign of ϕ in the Peierls substitution and hence

$$\mathcal{T}^{-1}\mathcal{H}^\phi(\mathbf{k})\mathcal{T} = \mathcal{H}^{-\phi}(-\mathbf{k}). \tag{5}$$

Let us first consider the simple case of $\Phi = 2\pi$, i.e., $n = 1$. Then ϕ is 2π periodic and behaves as k_z would in a 3D Hamiltonian. Furthermore, we recall that $H^{\phi+\Phi} = UH^\phi U^\dagger$, so from

$$(U\mathcal{T})H^\pi(U\mathcal{T})^\dagger = UH^{-\pi}U^\dagger = H^\pi \tag{6}$$

we see that $U\mathcal{T}$ is a symmetry of $H^{\phi=\pi}$. It can be shown that $(U\mathcal{T})^2 = \mathcal{T}^2 = -1$ [28], so H^π also has a $\mathbb{Z}_2$ topological classification. For pedagogical purposes, we assume that U is diagonal in momentum space. In the generic case, the algebra of $U\mathcal{T}$ and $T_i(\phi)$ acquires a projective phase that leads to an off-diagonal representation of $U\mathcal{T}$ on the magnetic BZ [28].

Considering H^ϕ as a 3D model with $\mathcal{T}$ symmetry, its topology is characterized by the magnetoelectric polarizability $\theta \in \{0, \pi\}$, where π is the nontrivial value of the 3D TI phase. θ is related to the Pfaffian $\mathbb{Z}_2$ invariants by $e^{i\theta} = \delta^{\phi=0} \times \delta^{\phi=\pi}$, where $\delta^\phi \in \{-1, 1\}$ is protected by $\mathcal{T}$ ($U\mathcal{T}$) at $\phi = 0$ (π) [39–41]. Because we assume that $H^{\phi=0}$ is nontrivial, we need only show that $\delta^{\phi=\pi} = +1$ in order to prove $\theta = \pi$. To do so, we introduce the parameter M, which tunes the H^ϕ to a trivial atomic limit as described in the previous section. Now consider the magnetic BZ at $\phi = \pi$ with $k_1 \in (-\pi, \pi), k_2 \in (0, \pi)$. Equation (4) requires the BZ to be π periodic, $\epsilon_m(\mathbf{k} + \pi\mathbf{b}_1) = \epsilon_m(\mathbf{k})$. As $M \to \infty$, we determine the change in $\delta^{\phi=\pi}$ by counting gap closings in *half* of the magnetic BZ defined by $BZ_{1/2} = k_1 \in (-\pi, \pi), k_2 \in (0, \pi/2)$ [40,42,43]. If there is a gap closing at $\mathbf{k}^* \in BZ_{1/2}$, there is a second identical closing at $\mathbf{k}^* + \pi\mathbf{b}_1 \in BZ_{1/2}$. Each gap closing changes the sign of $\delta^{\phi=\pi}$, so it must be that $\delta^{\pi=\phi} = +1$ because an even number of gap closings occur between $M = 0$ and the trivial phase at $M = \infty$. We conclude $\theta = \pi$, proving that the Hofstadter Hamiltonian is a 3D TI. On open boundary conditions (OBC), such a model will pump gapless edge states into the bulk as ϕ is increased, as exemplified in Fig. 1(b). There, for a perturbed model with only $\mathcal{T}$ symmetry H''_{QSH} [28], we observe gapless edge states for small flux and their disappearance into the bulk.

The π periodicity in the magnetic BZ was crucial to proving that $H^{\phi=\pi}$ is trivial. Generally, if $\Phi = 2\pi n$, then the $U\mathcal{T}$-symmetric point exists at $\Phi/2 = n\pi$. When n is odd, the energy spectrum is still π periodic along k_1, and we conclude that $\delta^{\phi=n\pi} = +1$ [28]. However when n is even, this π periodicity is absent, so our proof fails, and indeed, H^ϕ can be a weak or strong 3D TI [28].

Fragile topological insulators.—So far we have studied the Hofstadter topology deriving from strong topological 2D phases with a nontrivial Chern number, the mirror Chern number, or the $\mathbb{Z}_2$ index. We now consider a fragile invariant: the second Stiefel–Whitney index $w_2 \in \{0, 1\}$ protected by $C_{2z}\mathcal{T}$ [with $(C_{2z}\mathcal{T})^2 = +1$] [14,44–46].

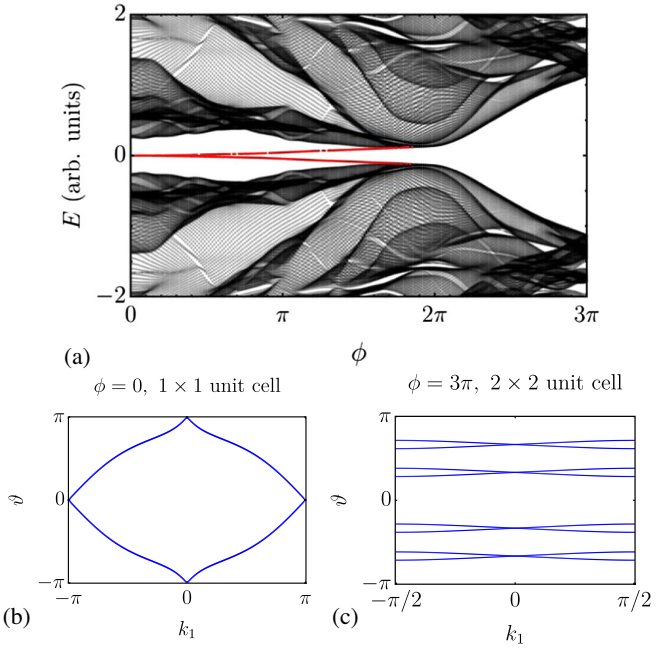

FIG. 2. Twisted bilayer graphene. (a) The Hofstadter Butterfly is calculated on a 30×30 lattice for H'_{TBG}, which has only $C_{2z}\mathcal{T}$ symmetry [28]. The corner modes are shown in red over the gapped black bulk and edge spectrum and pump between the nontrivial $w_2 = 1$ phase at $\phi = 0$ and the trivial phase at $\phi = 3\pi$, where $w_2 = 0$. This model is classified as a HOTI. (b) We observe from the Wilson loop spectrum, with eigenvalues $\exp i\vartheta(k_1)$, that $w_2^{\phi=0} = 1$ due to the odd number of crossings at $\vartheta = 0$ and $\vartheta = \pi$ [44]. (c) The Wilson spectrum at $\phi = 3\pi$ is calculated in an extended 2×2 unit cell where U is diagonal in momentum space [28]. Here, $w_2^{\phi=3\pi} = 0$ because there are no crossings at $\vartheta = 0$ and $\vartheta = \pi$.

A nontrivial value of $w_2 = 1$ indicates fractional corner states [44,47–50] and may be computed in the bulk from the Wilson loop eigenvalues or the nested Wilson loop [44,51,52].

The 3D HOTI phase is characterized by pumping corner states between a w_2 nontrivial phase and trivial phase [36,53]. Because $(C_{2z}\mathcal{T})^{-1}\mathcal{H}^{\phi}(\mathbf{k})(C_{2z}\mathcal{T}) = \mathcal{H}^{-\phi}(\mathbf{k})$, we can again identify ϕ with k_z and use 3D topological invariants to classify H^{ϕ}, which we now discuss.

We have assumed that $C_{2z}\mathcal{T}$ is a symmetry of $H^{\phi=0}$ and protects the invariant $w_2^{\phi=0}$. For a Hofstadter Hamiltonian that has a $\Phi = 2\pi n$ periodicity in flux, the other symmetric point occurs at $\phi = \Phi/2$ where $H^{\Phi/2}$ has the symmetry $UC_{2z}\mathcal{T}$. We can show that $(UC_{2z}\mathcal{T})^2 = \pm 1$, where the sign must be calculated from the Peierls paths [28]. The Hofstadter topological invariant depends on this sign. If $(UC_{2z}\mathcal{T})^2 = +1$, a nonzero value of $\theta/\pi = w_2^{\phi=0} - w_2^{\phi=\Phi/2}$ indicates corner state flow. The nontrivial phase with $\theta = \pi$ is a "strong" symmetry-protected topological phase with corner state pumping. [53–57].

If $(UC_{2z}\mathcal{T})^2 = -1$, there is no w_2 index at $\phi = \Phi/2$ [44]. However, we can diagnose the topology directly as a consequence of Kramers' theorem. Because $(UC_{2z}\mathcal{T})^2 = -1$, the states at C_{2z}-invariant positions must come in pairs at $\phi = \Phi/2$ and hence can always be removed from these positions without breaking the symmetry. Heuristically, these Kramers' pairs trivialize the bulk, and by the bulk-boundary correspondence, the model remains trivial with OBC [58–62]. This is confirmed explicitly by calculating the nested Wilson loop [28]. Thus, we find that $\theta/\pi = w_2^{\phi=0}$ only depends on the zero-field topology.

To exemplify the Hofstadter HOTI phase, we now consider H_{TBG}: a four-band model of TBG with C_{2x}, C_{3z}, C_{2z}, and $\mathcal{T}$ symmetries that possesses fragile Wilson loop winding yielding $w_2^{\phi=0} = 1$ [14,63]. We study a perturbed model H'_{TBG} that has only $C_{2z}\mathcal{T}$ to protect the fragile topology [28,64]. The Hofstadter Hamiltonian has $\Phi = 6\pi$ and $(UC_{2z}\mathcal{T})^2 = +1$ [28]. In Fig. 2(a), we calculate the Hofstadter Butterfly with OBC and observe the pumping of corner modes (with a gapped bulk and edge) that characterizes a HOTI. We show that $\theta = \pi$ by calculating the w_2 indices at $\phi = 0, \Phi/2$ from the Wilson loop spectra shown in Figs. 2(b) and 2(c) [28,65]. Breaking the C_{2z} and $C_{2x}\mathcal{T}$ symmetries of H_{TBG} (which are *not* true symmetries of TBG) is crucial. Both symmetries are preserved at all ϕ and can enforce a bulk gap closing [28,66–68], which would disrupt the appearance of the HOTI phase.

Discussion.—The topological phases of the Hofstadter Hamiltonian can be computed in the momentum-flux manifold. We demonstrated that a nonzero Chern number or mirror Chern number enforces a level crossing in the bulk as flux is pumped through the crystal. In analogy to the 3D classifications, we call this a topologically protected Hofstadter semimetal. The Hofstadter topology of a Hamiltonian with a nontrivial $\mathbb{Z}_2$ index depended on the flux periodicity $\Phi = 2\pi n$. When n is odd, we proved that the Hofstadter realized a 3D TI phase where the flux pumps edge states into the bulk. Finally, we considered fragile topology at zero flux given by nonzero w_2 index and found that the topological index of the Hofstadter Hamiltonian depended on the sign of $(UC_{2z}\mathcal{T})^2 = \pm 1$ through the Peierls paths. This is notably different from crystalline systems where $(C_{2z}\mathcal{T})^2 = +1$ with and without spin-orbit coupling. In the strong Hofstadter HOTI phase, realized by a model of TBG, the flux pumps corner states into the bulk.

We expect the results of this work to be experimentally verifiable using Moiré lattices, which have very large unit cells at small twist angles [19]. Indeed, after the submission of this work, Ref. [69] observed signatures of fragile Hofstadter topology in a TBG system, and Ref. [70] identified the flux-induced gap closings indicative of a Hofstadter semimetal protected by a valley Chern number in twisted double bilayer graphene. Both experiments show that realistic magnetic fields can probe the Hofstadter phase.

We thank Fang Xie, Biao Lian, Christopher Mora, and Benjamin Wieder for helpful discussions. We also thank one of our referees for pointing out Ref. [8]. B. A. B., N. R., and S. Z.-D. were supported by the Department of Energy Grant No. desc0016239, the Schmidt Fund for Innovative Research, Simons Investigator Grant No. 404513, and the Packard Foundation. Further support was provided by the National Science Foundation EAGER Grant No. DMR-1643312, NSF-MRSEC DMR-1420541, BSF Israel US foundation No. 2018226, and ONR No. N00014-20-1-2303.

J. H.-A. and Z.-D. S. contributed equally to this work.

Note added.—We point out a recent work, Ref. [13], which studies topological phase transitions in Hofstadter models by varying the parameters of the zero-field Hamiltonian.

[*] These authors contributed equally.

[1] D. R. Hofstadter, Energy levels and wave functions of Bloch electrons in rational and irrational magnetic fields, Phys. Rev. B **14**, 2239 (1976).

[2] D. J. Thouless, M. Kohmoto, M. P. Nightingale, and M. den Nij, Quantized Hall Conductance in a Two-Dimensional Periodic Potential, Phys. Rev. Lett. **49**, 405 (1982).

[3] P. G. Harper, The general motion of conduction electrons in a uniform magnetic field, with application to the diamagnetism of metals, Proc. Phys. Soc. London Sect. A **68**, 879 (1955).

[4] G. Naumis, Higher-dimensional quasicrystalline approach to the Hofstadter Butterfly topological-phase band conductances: Symbolic sequences and self-similar rules at all magnetic fluxes, Phys. Rev. B **100**, 165101 (2019).

[5] B. A. Bernevig and T. L. Hughes, *Topological Insulators and Topological Superconductors*, Student edition (Princeton University Press, Princeton, NJ, 2013), ISBN .

[6] P. Wang, B. Cheng, O. Martynov, T. Miao, L. Jing, T. Taniguchi, K. Watanabe, V. Aji, C. N. Lau, and M. Bockrath, Topological winding number change and broken inversion symmetry in a Hofstadter's Butterfly, Nano Lett. **15**, 6395 (2015).

[7] C. Albrecht, J. H. Smet, K. von Klitzing, D. Weiss, V. Umansky, and H. Schweizer, Evidence of Hofstadter's Fractal Energy Spectrum in the Quantized Hall Conductance, Phys. Rev. Lett. **86**, 147 (2001).

[8] I. Dana, Y. Avron, and J. Zak, Quantised Hall conductance in a perfect crystal, J. Phys. C **18**, L679 (1985).

[9] Y. Otaki and T. Fukui, Higher-order topological insulators in a magnetic field, Phys. Rev. B **100**, 245108 (2019).

[10] Y. Deng, Y. Yu, M. Zhu Shi, Z. Guo, Z. Xu, J. Wang, X. H. Chen, and Y. Zhang, Quantum anomalous Hall effect in intrinsic magnetic topological insulator $MnBi_2Te_4$, Science **367**, 895 (2020).

[11] C.-Z. Chang *et al.*, Experimental observation of the quantum anomalous Hall effect in a magnetic topological insulator, Science **340**, 167 (2013).

[12] P. Cheng *et al.*, Landau Quantization of Topological Surface States in Bi_2Se_3, Phys. Rev. Lett. **105**, 076801 (2010).

[13] J. Wang and L. H. Santos, following Letter, Classification of Topological Phase Transitions and van Hove Singularity Steering Mechanism in Graphene Superlattices, Phys. Rev. Lett. **125**, 236805 (2020).

[14] Z.-D. Song, Z. Wang, W. Shi, G. Li, C. Fang, and B. A. Bernevig, All Magic Angles in Twisted Bilayer Graphene are Topological, Phys. Rev. Lett. **123**, 036401 (2019).

[15] X. Ni, K. Chen, M. Weiner, D. J. Apigo, C. Prodan, A. Alù, E. Prodan, and A. B. Khanikaev, Observation of Hofstadter Butterfly and topological edge states in reconfigurable quasi-periodic acoustic crystals, Commun. Phys. **2**, 55 (2019).

[16] C. R. Dean, L. Wang, P. Maher, C. Forsythe, F. Ghahari, Y. Gao, J. Katoch, M. Ishigami, P. Moon, M. Koshino, T. Taniguchi, K. Watanabe, K. L. Shepard, J. Hone, and P. Kim, Hofstadter's Butterfly and the fractal quantum Hall effect in Moiré superlattices, Nature (London) **497**, 598 (2013).

[17] B. Hunt, J. D. Sanchez-Yamagishi, A. F. Young, M. Yankowitz, B. J. LeRoy, K. Watanabe, T. Taniguchi, P. Moon, M. Koshino, and P. Jarillo-Herrero, Massive dirac fermions and Hofstadter Butterfly in a van der Waals heterostructure, Science **340**, 1427 (2013).

[18] L. A. Ponomarenko, R. V. Gorbachev, G. L. Yu, D. C. Elias, R. Jalil, A. A. Patel, A. Mishchenko, A. S. Mayorov, C. R. Woods, and J. R. Wallbank, Cloning of Dirac fermions in graphene superlattices, Nature (London) **497**, 594 (2013).

[19] R. Bistritzer and A. H. MacDonald, Moiré bands in twisted double-layer graphene, Proc. Natl. Acad. Sci. U.S.A. **108**, 12233 (2011).

[20] C. R. Dean, A. F. Young, I. Meric, C. Lee, L. Wang, S. Sorgenfrei, K. Watanabe, T. Taniguchi, P. Kim, K. L. Shepard, and J. Hone, Boron nitride substrates for high-quality graphene electronics, Nat. Nanotechnol. **5**, 722 (2010).

[21] Y. Cao, V. Fatemi, A. Demir, S. Fang, S. L. Tomarken, J. Y. Luo, J. D. Sanchez-Yamagishi, K. Watanabe, T. Taniguchi, E. Kaxiras, R. C. Ashoori, and P. Jarillo-Herrero, Correlated insulator behaviour at half-filling in magic-angle graphene superlattices, Nature (London) **556**, 80 (2018).

[22] Y. Xie, B. Lian, B. Jäck, X. Liu, C.-L. Chiu, K. Watanabe, T. Taniguchi, B. A. Bernevig, and A. Yazdani, Spectroscopic signatures of many-body correlations in magic-angle twisted bilayer graphene, Nature (London) **572**, 101 (2019).

[23] V. A. Skachkova, M. S. Baranava, D. C. Hvazdouski, and V. R. Stempitsky, Electronic properties of graphene-based heterostructures, J. Phys. Conf. Ser. **917**, 092012 (2017).

[24] I. Meric, C. R. Dean, A. F. Young, J. Hone, P. Kim, and K. L. Shepard, Graphene field-effect transistors based on boron nitride gate dielectrics, arXiv:1101.4712.

[25] B. Hunt, J. D. Sanchez-Yamagishi, A. F. Young, M. Yankowitz, B. J. LeRoy, K. Watanabe, T. Taniguchi, P. Moon, M. Koshino, P. Jarillo-Herrero, and R. C. Ashoori, Massive dirac fermions and Hofstadter Butterfly in a van der Waals heterostructure, Science **340**, 1427 (2013).

[26] I. Meric, C. R. Dean, A. F. Young, J. Hone, P. Kim, and K. L. Shepard, Graphene field-effect transistors based on boron nitride gate dielectrics, IEEE IEDM Tech. Dig. 556 (2010).

[27] R. Peierls, Zur Theorie des Diamagnetismus von Leitungselektronen, Z. Phys. **80**, 763 (1933).

[28] See Supplemental Material at http://link.aps.org/supplemental/10.1103/PhysRevLett.125.236804 for a description of additional calculations.

[29] J. Zak, Magnetic translation group, Phys. Rev. **134**, A1602 (1964).

[30] K. Sun, Z. Gu, H. Katsura, and S. Das Sarma, Nearly Flatbands with Nontrivial Topology, Phys. Rev. Lett. **106**, 236803 (2011).

[31] B. A. Bernevig and N. Regnault, Emergent many-body translational symmetries of Abelian and non-Abelian fractionally filled topological insulators, Phys. Rev. B **85**, 075128 (2012).

[32] Note that the structure of an on-site potential is identical for the q unit cells within the magnetic unit cell.

[33] S. A. Parameswaran, R. Roy, and S. L. Sondhi, Fractional quantum Hall physics in topological flat bands, C.R. Phys. **14**, 816 (2013).

[34] C. Brouder, G. Panati, M. Calandra, C. Mourougane, and N. Marzari, Exponential Localization of Wannier Functions in Insulators, Phys. Rev. Lett. **98**, 046402 (2007).

[35] B. A. Bernevig, T. L. Hughes, and S.-C. Zhang, Quantum spin Hall effect and topological phase transition in HgTe quantum wells, Science **314**, 1757 (2006).

[36] F. Schindler, A. M. Cook, M. G. Vergniory, Z. Wang, S. S. P. Parkin, B. A. Bernevig, and T. Neupert, Higher-order topological insulators, Sci. Adv. **4**, eaat0346 (2018).

[37] A. Kitaev, in *Periodic Table for Topological Insulators and Superconductors*, edited by V. Lebedev and M. Feigel'Man, American Institute of Physics Conference Series, Vol. 1134 of American Institute of Physics Conference Series (2009), pp. 22–30, https://doi.org/10.1063/1.3149495.

[38] S. Ryu, A. P. Schnyder, A. Furusaki, and A. W. W. Ludwig, Topological insulators and superconductors: Tenfold way and dimensional hierarchy, New J. Phys. **12**, 065010 (2010).

[39] L. Fu, C. L. Kane, and E. J. Mele, Topological Insulators in Three Dimensions, Phys. Rev. Lett. **98**, 106803 (2007).

[40] C. L. Kane and E. J. Mele, Z_2 Topological Order and the Quantum Spin Hall Effect, Phys. Rev. Lett. **95**, 146802 (2005).

[41] R. Yu, X. Liang Qi, A. Bernevig, Z. Fang, and X. Dai, Equivalent expression of Z_2 topological invariant for band insulators using the non-Abelian Berry connection, Phys. Rev. B **84**, 075119 (2011).

[42] R. Roy, Topological phases and the quantum spin Hall effect in three dimensions, Phys. Rev. B **79**, 195322 (2009).

[43] L. Fu and C. L. Kane, Time reversal polarization and a Z_2 adiabatic spin pump, Phys. Rev. B **74**, 195312 (2006).

[44] J. Ahn, S. Park, and B.-J. Yang, Failure of Nielsen-Ninomiya Theorem and Fragile Topology in Two-Dimensional Systems with Space-Time Inversion Symmetry: Application to Twisted Bilayer Graphene at Magic Angle, Phys. Rev. X **9**, 021013 (2019).

[45] H. Chun Po, L. Zou, T. Senthil, and A. Vishwanath, Faithful tight-binding models and fragile topology of magic-angle bilayer graphene, Phys. Rev. B **99**, 195455 (2019).

[46] Z. Wang, B. J. Wieder, J. Li, B. Yan, and B. A. Bernevig, Higher-Order Topology, Monopole Nodal Lines, and the Origin of Large Fermi Arcs in Transition Metal Dichalcogenides XTe_2 (X = Mo, W), Phys. Rev. Lett. **123**, 186401 (2019).

[47] Z. Song, L. Elcoro, N. Regnault, and B. A. Bernevig, Fragile Phases as Affine Monoids: Classification and Material Examples, Phys. Rev. X **10**, 031001 (2020).

[48] A. Bouhon, A. M. Black-Schaffer, and R.-J. Slager, Wilson loop approach to fragile topology of split elementary band representations and topological crystalline insulators with time-reversal symmetry, Phys. Rev. B **100**, 195135 (2019).

[49] Z.-D. Song, Z. Fang, and C. Fang, $(d-2)$-Dimensional Edge States of Rotation Symmetry Protected Topological States, Phys. Rev. Lett. **119**, 246402 (2017).

[50] W. A. Benalcazar, B. A. Bernevig, and T. L. Hughes, Quantized electric multipole insulators, Science **357**, 61 (2017).

[51] W. A. Benalcazar, B. A. Bernevig, and T. L. Hughes, Electric multipole moments, topological multipole moment pumping, and chiral hinge states in crystalline insulators, Phys. Rev. B **96**, 245115 (2017).

[52] A. Alexandradinata, X. Dai, and B. A. Bernevig, Wilson-loop characterization of inversion-symmetric topological insulators, Phys. Rev. B **89**, 155114 (2014).

[53] B. J. Wieder and B. A. Bernevig, The axion insulator as a pump of fragile topology, arXiv:1810.02373.

[54] If both $w_2^{\phi=0} = w_2^{\phi=\Phi/2} = 1$, then $\theta = 0$ but both $H^{\phi=0}$ and $H^{\phi=\Phi/2}$ have nontrivial corner states, which is a "weak" 3D fragile state.

[55] M. I. Aroyo, J. M. Perez-Mato, C. Capillas, E. Kroumova, S. Ivantchev, G. Madariaga, A. Kirov, and H. Wondratschek, Bilbao crystallographic server: I. Databases and crystallographic computing programs, Z. Kristallogr. **221**, 15 (2006).

[56] M. I. Aroyo, A. Kirov, C. Capillas, J. M. Perez-Mato, and H. Wondratschek, Bilbao crystallographic server. II. Representations of crystallographic point groups and space groups, Acta Crystallogr. Sect. A **62**, 115 (2006).

[57] J. Herzog-Arbeitman, Z. Song, and A. Bernevig, Symmetry-protected Hofstadter topology: Signatures of the fragile phase (to be published).

[58] Z.-D. Song, L. Elcoro, and B. A. Bernevig, Twisted bulk-boundary correspondence of fragile topology, Science **367**, 794 (2020).

[59] E. Khalaf, H. Chun Po, A. Vishwanath, and H. Watanabe, Symmetry Indicators and Anomalous Surface States of Topological Crystalline Insulators, Phys. Rev. X **8**, 031070 (2018).

[60] M. Geier, L. Trifunovic, M. Hoskam, and P. W. Brouwer, Second-order topological insulators and superconductors with an order-two crystalline symmetry, Phys. Rev. B **97**, 205135 (2018).

[61] L. Trifunovic and P. W. Brouwer, Higher-Order Bulk-Boundary Correspondence for Topological Crystalline Phases, Phys. Rev. X **9**, 011012 (2019).

[62] E. Khalaf, Higher-order topological insulators and superconductors protected by inversion symmetry, Phys. Rev. B **97**, 205136 (2018).

[63] B. Lian, F. Xie, and B. A. Bernevig, The Landau level of fragile topology, Phys. Rev. B **102**, 041402 (2020).

[64] T. L. Hughes, E. Prodan, and B. A. Bernevig, Inversion-symmetric topological insulators, Phys. Rev. B **83**, 245132 (2011).

[65] At $\Phi/2$, we have artificially doubled the magnetic unit cell along the $\mathbf{a}_1$ direction so that $UC_{2z}\mathcal{T}$ is diagonal in momentum space.

[66] B. Bradlyn, L. Elcoro, J. Cano, M. G. Vergniory, Z. Wang, C. Felser, M. I. Aroyo, and B. A. Bernevig, Topological quantum chemistry, Nature (London) **547**, 298 (2017).

[67] J. Cano, B. Bradlyn, Z. Wang, L. Elcoro, M. G. Vergniory, C. Felser, M. I. Aroyo, and B. A. Bernevig, Building blocks of topological quantum chemistry: Elementary band representations, Phys. Rev. B **97**, 035139 (2018).

[68] M. G. Vergniory, L. Elcoro, Z. Wang, J. Cano, C. Felser, M. I. Aroyo, B. A. Bernevig, and B. Bradlyn, Graph theory data for topological quantum chemistry, Phys. Rev. E **96**, 023310 (2017).

[69] X. Lu, B. Lian, G. Chaudhary, B. A. Piot, G. Romagnoli, K. Watanabe, T. Taniguchi, M. Poggio, A. H. MacDonald, B. A. Bernevig, and D. K. Efetov, Fingerprints of fragile topology in the Hofstadter spectrum of twisted bilayer graphene close to the second magic angle, arXiv: 2006.13963.

[70] G. William Burg, B. Lian, T. Taniguchi, K. Watanabe, B. A. Bernevig, and E. Tutuc, Evidence of emergent symmetry and valley chern number in twisted double-bilayer graphene, arXiv:2006.14000.